

Alyssa C. Henry  
Emanuel A. Waddell  
Rubina Shreiner  
Laurie E. Locascio

Analytical Chemistry Division,  
National Institute of Standards  
and Technology,  
Gaithersburg, MD, USA

## Control of electroosmotic flow in laser-ablated and chemically modified hot imprinted poly(ethylene terephthalate glycol) microchannels

The fabrication of microchannels in poly(ethylene terephthalate glycol) (PETG) by laser ablation and the hot imprinting method is described. In addition, hot imprinted microchannels were hydrolyzed to yield additional charged organic functional groups on the imprinted surface. The charged groups are carboxylate moieties that were also used as a means for the further reaction of different chemical species on the surface of the PETG microchannels. The microchannels were characterized by fluorescence mapping and electroosmotic flow (EOF) measurements. Experimental results demonstrated that different fabrication and channel treatment protocols resulted in different EOF rates. Laser-ablated channels had similar EOF rates ( $5.3 \pm 0.3 \times 10^{-4} \text{ cm}^2/\text{Vs}$  and  $5.6 \pm 0.4 \times 10^{-4} \text{ cm}^2/\text{Vs}$ ) to hydrolyzed imprinted channels ( $5.1 \pm 0.4 \times 10^{-4} \text{ cm}^2/\text{Vs}$ ), which in turn demonstrated a somewhat higher flow rate than imprinted PETG channels that were not hydrolyzed ( $3.5 \pm 0.3 \times 10^{-4} \text{ cm}^2/\text{Vs}$ ). Laser-ablated channels that had been chemically modified to yield amines displayed an EOF rate of  $3.38 \pm 0.1 \times 10^{-4} \text{ cm}^2/\text{Vs}$  and hydrolyzed imprinted channels that had been chemically derivatized to yield amines showed an EOF rate of  $2.67 \pm 0.6 \text{ cm}^2/\text{Vs}$ . These data demonstrate that surface-bound carboxylate species can be used as a template for further chemical reactions in addition to changing the EOF mobility within microchannels.

**Keywords:** Imprinting / Laser ablation / Micromachining / Poly(ethylene terephthalate glycol) / Surface chemical modification  
EL 4815

### 1 Introduction

There has recently been a thrust to miniaturize several workhorses of analytical chemistry including capillary electrophoresis (CE) [1–4] and mass spectrometry (MS) [5, 6]. Interest in the miniaturization of many bioanalytical techniques has increased due to a reduction in time, reagents, and space required to perform analyses. For example, researchers have performed the polymerase chain reaction [7], oligonucleotide hybridization [8], illicit drug identification [9], and DNA sequencing [10] in miniaturized systems, commonly known as lab-on-a-chip (LOC) or micrototal analysis systems ( $\mu\text{TAS}$ ). In these instances, electrophoretic separations are generally performed in micrometer sized channels fabricated in planar substrates.

Traditionally,  $\mu\text{TAS}$  have been fabricated in glass due to its well documented modification chemistries and the ability

**Correspondence:** Dr. Laurie E. Locascio, Analytical Chemistry Division, National Institute of Standards and Technology, Gaithersburg, MD, 20899-8394, USA  
**E-mail:** laurie.locascio@nist.gov  
**Fax:** +301-977-0587

**Abbreviations:** AF, 5-(aminoacetamido)fluorescein; EDC, 1-ethyl-3-(3-dimethylaminopropyl carbodiimide); PET, poly(ethylene terephthalate); PETG, poly(ethylene terephthalate glycol)

to transfer separation conditions from a silica capillary to silica-based  $\mu\text{TAS}$  [11, 12]. However, there has recently been increased interest in using polymer substrates in the fabrication of  $\mu\text{TAS}$ . Polymer substrates are of interest because of the low cost associated with many thermoplastics and the multiple methods by which  $\mu\text{TAS}$  may be fabricated from polymeric materials. Polymeric microchannels can be fabricated by a number of techniques, including mask lithography [13], injection molding [10], imprinting [14, 15], embossing [16, 17], and laser ablation [18]. In addition to the number of methods available for channel fabrication, the assembly of polymeric devices is a facile process. In the bonding or sealing step of device assembly, a top plate may be heat sealed to the plate containing the microchannel [14]. The low glass transition temperature ( $T_g$ ) of polymers allows for the relatively low assembly temperatures as compared to the high ( $> 600^\circ\text{C}$ ) assembly temperatures needed for silica-based devices [19]. A disadvantage associated with polymer microchannels, however, is that the surface chemistries of many polymers are not well understood.

The control of the surface chemistry is important due to the dependence of the electroosmotic flow (EOF) on the magnitude of the microchannel surface charge. In the case of a silica capillary, the surface of the capillary is negatively charged, and the flow of the bulk solution is

directed from the anode to the cathode with the velocity dependent upon the number of dissociated silanol groups on the wall of the capillary. Because this system is well characterized, it is straightforward to adjust the experimental conditions and predict the result. Much less is known about polymer substrates as supports for EOF [20], although there have been recent reports in the literature that demonstrate that the EOF may be controlled *via* chemical surface modifications [11], alteration of the channel surface by exposure to excimer radiation [21], or coating the channel wall with materials such as polyelectrolyte multilayers (PEMS) [22, 23]. In addition, recent reports have also demonstrated that the fabrication of microchannels by laser ablation techniques results in surface organic functional groups that are different from those present on the pristine plastic; thus, the EOF may be manipulated simply by fabricating the microchannel using laser ablation [24, 25]. The control of the EOF allows one to tailor microfluidic channels for specific applications such as DNA sequencing, which optimally requires a reduced EOF.

In this report, we describe and compare the control of EOF in poly(ethylene terephthalate glycol) (PETG) microchannels using chemical surface modification and laser ablation under various atmospheric conditions. PETG is utilized as the substrate material for these modifications because it is an amenable substrate for imprinting and laser ablation, and it is approved for use in biomedical devices. The goal of this work is to demonstrate that the control of EOF in common plastics, such as PETG, may be accomplished by simple techniques.

## 2 Materials and methods

### 2.1 Chemicals

PETG sheets were obtained from DSM Engineering Plastic Products (Sheffield, MA, USA). 5-(Aminoacetamido) fluorescein (fluoresceinyl glycine amide) (AF) was purchased from Molecular Probes (Eugene, OR, USA). The water-soluble carbodiimide used in the coupling experiments was 1-ethyl-3-(3-dimethylaminopropyl) carbodiimide (EDC; Sigma, St. Louis, MO, USA) and was used as received. *N*-Methyl-1,3-propane diamine was purchased from Aldrich (Milwaukee, WI, USA). Triply distilled water was obtained from a Milli-Q distillation system and used without filtering. The phosphate buffer, which was used for the current monitoring experiments, was prepared from potassium dihydrogenphosphate and disodium hydrogen phosphate (Sigma-Aldrich). Sodium hydroxide (NaOH) was dissolved in distilled water to prepare a 5 M solution.

### 2.2 Fabrication of imprinted channels

Imprinted channels were fabricated using the silicon micromachined template hot imprinting method described elsewhere [14]. Briefly, a silicon wafer was etched to produce a raised three-dimensional image of 30  $\mu\text{m}$  deep trapezoidal channels. The PETG substrate was then placed between the silicon wafer and a glass slide. The glass slide/PETG substrate/silicon template assembly was positioned between polished aluminum blocks and heated to 80°C at a pressure of 3.4 MPa (500 psi) for 20 min. After cooling to room temperature, the substrate was removed from between the template and the glass slide. Hydrolysis of PETG sheets consisted of immersing the PETG sheets in 5 M NaOH solution for 2 h to hydrolyze the polyester backbone of the polymer. Alternatively, assembled channels were hydrolyzed by flushing NaOH solution through the imprinted microchannels for 10 min using vacuum suction. Chemical modification of hydrolyzed and ablated PETG channels to produce surface-bound amines was performed using EDC as a coupling agent, and surface-bound carboxylate groups and *N*-Methyl-1,3-propane diamine as reactants. Briefly, a 0.5 mM EDC solution was prepared in 100 mM phosphate buffer (pH 7.3). The solution, along with the PETG sheet, was placed in an airtight vessel and purged for 1 h with nitrogen. *N*-Methyl-1,3-propane diamine was added, by cannula or syringe, to the purged, sealed vessel such that a final concentration of 0.5 mM was attained. The reaction was allowed to proceed for 2 h under a constant nitrogen purge. After 2 h, the PETG piece was removed from the reaction vessel and rinsed three times with phosphate buffer (pH 7.3) and three times with triply distilled water. The PETG piece was then blown dry under a stream of nitrogen.

### 2.3 Fabrication of laser-ablated channels

To fabricate laser-ablated channels, we utilized a commercial laser ablation system (LMT-4000 Laser Micromachining System, Potomac Photonics, Lanham, MD, USA) that was equipped with a KrF pulsed (7 ns) excimer (248 nm) laser and a PC-based motion controller (Aerotech Unidex 500; Pittsburgh, PA, USA). In Fig. 1 a schematic of the laser ablation system is displayed. A KrF excimer laser emits pulses of 248 nm photons that are passed through a beam defining aperture (1) and steered by a dichroic (2) through the focusing objective (3). It was possible to control the repetition rate of the laser from single shot to 200 Hz. The polymer substrate (4) was vacuum mounted on a computer controlled *x-y* stage that had a  $\pm 1$   $\mu\text{m}$  repeatability (5). The surface of the

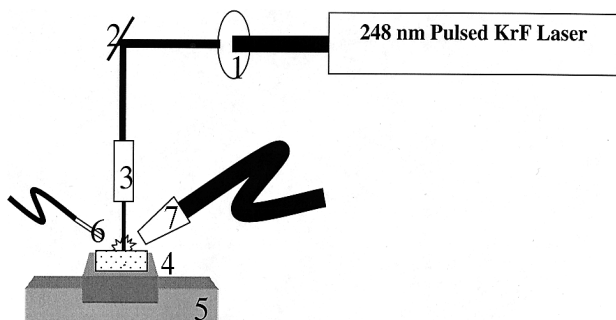


**Figure 1.** Schematic of the laser ablation micromachining system. A KrF excimer laser emits pulses of 248 nm photons that are passed through a beam defining aperture (1) and steered by a dichroic (2) through the focusing objective (3). The polymer substrate (4) is vacuum-mounted on a computer controlled *x-y* stage (5). The surface of the substrate may be exposed to various gases *via* nozzle (6) and the vacuum nozzle (7) assists in removal of large debris. The entire process is illuminated with a light source and imaged with a camera (not shown).

substrate was exposed to various gases *via* nozzle (6). The pressure of the gas exiting the nozzle was 0.1 MPa (20 psi) and was controlled with the use of a gas regulator. The vacuum nozzle (7) was used to assist in removal of large debris. The entire process was illuminated with a light source and imaged with a camera (not shown). The oxygen sweep gas used during ablation was 99.9% pure and was obtained from MG Industries (Frederick, MD, USA), and the nitrogen sweep gas was obtained from a liquid nitrogen boil-off.

The top piece of the microdevice was fabricated by drilling two 3 mm holes 1.8 cm apart in a second PETG substrate and placing it between two glass slides. The glass slide/PETG substrate/glass slide assembly was situated between two polished aluminum blocks for 10 min at 75°C. The PETG top piece was removed from between the two glass slides and was then ready for thermal bonding to the channel-imprinted PETG substrate. The PETG top piece and channel-imprinted substrate were thermally bonded by clamping the plastic pieces together between microscope slides and placing the assembly in a circulating air oven at 75°C for 10 min. The bonded device was then allowed to cool to room temperature for 5 min before the clamps were released. It is important to note that, in the case of the laser ablated devices, the top piece of the device is pristine PETG. Scanning electron microscopy images were obtained using a Hitachi S4500 Field Emission Gun (FEM) Scanning Electron Microscope (SEM). The microscope was operated with an accelerat-

ing voltage of 20 kV. The specimens were mounted with carbon tape and coated with approximately 10 nm carbon before imaging.

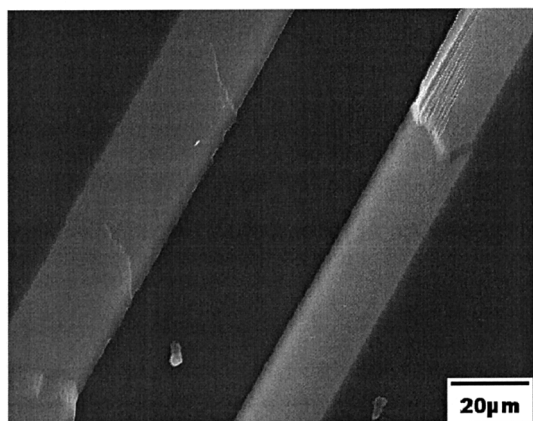
## 2.4 Chemical mapping

The chemical mapping technique has been described previously by this group [26, 27]. This technique utilizes group-specific, fluorescent probes to indicate the presence of active chemical functionalities on the surface. In this work, EDC was used as a coupling agent in the reaction of surface-bound carboxylic acid groups with the amine functionality on the AF. Thus, a fluorescent image of a surface indicates the presence of carboxylic acids on the PETG (imprinted, hydrolyzed imprinted, or ablated) surface. Fluorescence images were obtained using a Zeiss Axioplan 2 Microscope (Thornwood, NY, USA) equipped with a mercury arc excitation lamp and a fluorescein filter set. The images were collected using a CCD camera, and recorded using framegrabber software on a personal computer. The background was subtracted from each image.

## 2.5 Monitoring

The apparatus for the current monitoring method has also been reported elsewhere [28]. In brief, the microchannel was filled *via* vacuum with a 20 mM, pH 7.3 (107 mM ionic strength) phosphate buffer. Platinum electrodes were placed in each well and the current was monitored through the channel by measuring the voltage drop across a 100 k $\Omega$  resistor using an A/D converter. After attaining a steady current, the wells of the device were depleted of existing solution and equal aliquots of 10 mM, pH 7.3 phosphate buffer (53.7 mM ionic strength) and 20 mM, pH 7.3 phosphate buffer (107 mM ionic strength) were placed separately in the two wells. The power supply was immediately turned on and the voltage drop was monitored until a steady state was again reached. The wells were again depleted of existing solution and refilled with equal aliquots of 20 mM, pH 7 phosphate buffer (107 mM ionic strength) and the entire process repeated. Measurements were performed at 200, 300, 400, 500, and 600 V. The amount of time required to fill the channel was calculated at each voltage, using in-house software, and the resulting EOF rate was determined. The electroosmotic mobility was calculated by taking the ratio of the EOF and the electric field strength and averaging the data from measurements made at the various voltages. This is a bulk flow method and although it provides good information on average flow rates in the channel, it cannot readily be used to assess properties such as dispersion.

A.



B.

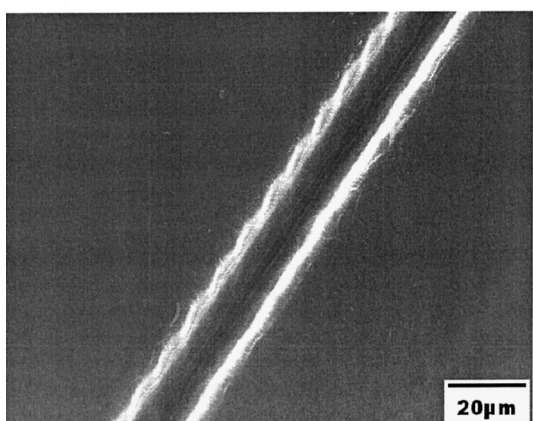


**Figure 2.** Representative scanning electron micrographs of (A) a channel fabricated by means of hot imprinting and (B) a channel fabricated by means of laser ablation under nitrogen.

### 3 Results and discussion

#### 3.1 Morphological characteristics of imprinted and laser-ablated PETG microchannels

Representative scanning electron micrographs of PETG channels fabricated by hot imprinting and laser ablation methods are displayed in Fig. 2. In Fig. 2A a channel fabricated by means of the imprinting method is shown. The channel walls are relatively smooth and appear, for the most part, featureless. In Fig. 2B a representative scanning electron micrograph of a PETG channel manufactured using laser ablation is depicted. In contrast to the imprinted channel, the ablated channel is rough and displays ridges on its walls and bottom that are due to the pulsed laser ablation process. In addition to the ridged features on the channel, bright features at the top of the walls of the channel are noted. This bright, lined feature is most likely due to the presence of ablated

PETG byproducts deposited on the top, inside wall of the channel. The increased overall surface roughness of the ablated channels as opposed to imprinted channels is expected due to the rapid thermal expansion and resulting pressure explosion that occurs during laser ablation of polymer substrates. It was previously reported that ablated poly(ethylene terephthalate) (PET), a similar material, has a much higher surface roughness than the nonablated polymer surface as determined by atomic force microscopy [18]

#### 3.2 Chemical modification of PETG-imprinted channel surfaces by base hydrolysis

The chemical modification of PETG was accomplished by base hydrolysis (NaOH) of the polyester backbone as shown in Fig. 3. After hydrolysis of the polyester, a number of chemical moieties may be present on the surface of the PETG, specifically hydroxyls and/or carboxylate moieties. Previous work has noted that the base hydrolysis of PET is a surface-bound process. That is, exposure of amorphous PET to base yields hydrolyzed products on the surface of the polymer rather than in the bulk polymer. One explanation for this phenomenon stems from the fact that the surface-bound products formed during hydrolysis, such as hydroxyl and carboxylate moieties, are negatively charged (deprotonated) at the high pH values required for base hydrolysis. Because the hydroxyl ions of the base are also negatively charged, electrostatic repulsion prevents the hydroxyl species from further hydrolyzing the bulk polymer. In the case of PETG, the base monomeric unit of PETG is the same as PET; the difference in the two polymers lies in the stabilizing reagents added to PETG [24]. As a result, hydrolysis of PETG should also be a surface selective process.

In Fig. 4 fluorescence intensity profiles of several PETG surfaces exposed to AF in the presence of EDC in pH 7.3 phosphate buffer are displayed. In this reaction, the amine moiety in the AF compound will react, in the presence of a coupling agent (EDC), with carboxylate moieties present on the surface of the PETG. In the case of pristine PETG, the average fluorescence intensity is low, ~276 fluorescence units, indicating a small amount of surface-bound carboxylate groups. In contrast, the average fluorescence intensity of the COO-PETG surface exposed to the same fluorescein compound and coupling agent is significantly higher, ~350 fluorescence units. This is due to the increased presence of carboxylate moieties on the surface of the hydrolyzed PETG. In addition, the fluorescence intensity plot appears fairly consistent and is the same shape as that of the pristine PETG, indicating that the hydrolysis procedure yields a homogeneous COO-PETG surface. It must be noted that, in addi-

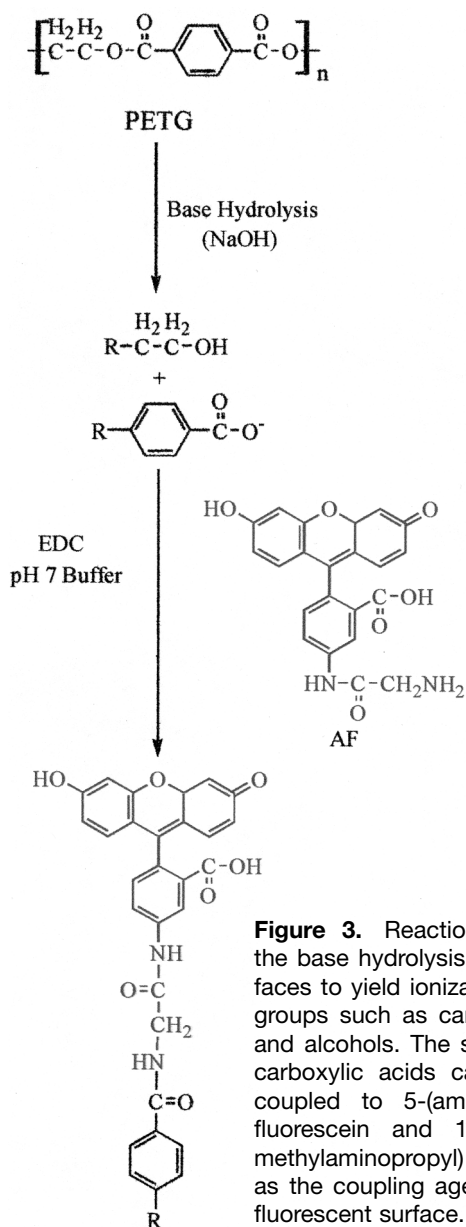


**Figure 3.** Reaction scheme of the base hydrolysis of PETG surfaces to yield ionizable functional groups such as carboxylic acids and alcohols. The surface-bound carboxylic acids can be further coupled to 5-(aminoacetamido) fluorescein and 1-ethyl-3-(3-dimethylaminopropyl) carbodiimide as the coupling agent, yielding a fluorescent surface.

tion to carboxylates, hydroxyl moieties can also be present on the surface of the hydrolyzed PETG; however, the fluorescein coupling reagents that were used do not bind to or detect hydroxyl groups. The possible presence of hydroxyls on the surface of the PETG is under investigation.

Functional groups such as carboxylates that may be present on the PETG after hydrolysis are easy to ionize in buffers with pH values similar to or higher than the  $\text{pK}_a$  of the carboxylate. In contrast, the ester groups of the PETG backbone are not easily ionizable; thus, one would expect a higher surface charge on the hydrolyzed PETG surface as opposed to the pristine PETG surface. These surface

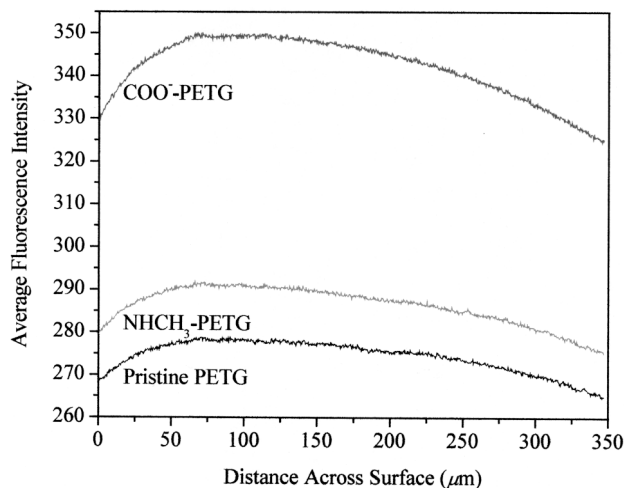


**Figure 4.** Representative fluorescence intensity profiles of the pristine PETG, COO-PETG, and NHCH<sub>3</sub>-PETG surfaces exposed to 5-(aminoacetamido) fluorescein and 1-ethyl-3-(3-dimethylaminopropyl) carbodiimide as the coupling agent.

charges are responsible for propagating the EOF of bulk solution through a plastic microchannel. As a result, one would expect that a PETG microchannel that is not hydrolyzed would have a slower EOF mobility than a hydrolyzed PETG channel. At pH 7.3, the average EOF mobility in imprinted PETG microchannels was determined to be  $3.5 \pm 0.3 \times 10^{-4} \text{ cm}^2/\text{Vs}$ . This value for EOF mobility is approximately an order of magnitude greater than the value reported by Morris *et al.* [29] in channels that were fabricated with the hot wire imprinting method. The EOF mobility reported here is approximately the same as that reported by Locascio and co-workers [23] in a previous study. In all cases, the plastic was obtained from the same manufacturer. The differences in the EOF mobilities reported by the two groups could be due to the batch-to-batch synthetic and/or packaging variations in the plastic material. That is, differences in various materials or the amounts of materials added to the plastic as stabilizers, UV masking agents, *etc.* may account for the dissimilarity between the EOF mobility values.

The base-hydrolyzed PETG, COO-PETG, channel yielded an EOF mobility value greater than that of the non-hydrolyzed PETG channel. The EOF mobility of the COO-PETG channel was determined to be  $5.1 \pm 0.4 \times 10^{-4} \text{ cm}^2/\text{Vs}$ . The difference in the EOF mobility of the COO-PETG channel *versus* the native PETG channel was approximately 1.5-fold. It is important to note that this value was only obtained when the assembled channel was hydrolyzed. That is, NaOH solution was pumped through an assembled PETG channel in order to hydrolyze the ester backbone of the channel walls. An alternative approach

was to hydrolyze the channel plate and the top plate before assembly. When devices were assembled in this fashion, they delaminated, often during use. It is likely that the electrostatic repulsion of the negative charges on the two pieces of plastic prevented proper adhesion between the channel plate and the top plate. Further experiments are necessary to determine the conditions for channel assembly after hydrolysis of the bulk substrate material.

### 3.3 Chemical modification of hydrolyzed PETG to yield amine-terminated PETG microchannels

Aside from altering the EOF, the presence of additional carboxylate species on the hydrolyzed PETG allows for further chemical reactions; that is, coupling reactions between the surface-bound carboxylate species and primary amines. In Fig. 5 a reaction scheme involving the surface-bound carboxylates and *N*-methyl-1,3-propane diamine is shown. In the case where the entire surface is successfully reacted, the EOF should run from cathode to anode due to the presence of a positive charge on the surface-bound secondary amine (at pH 7.3). This EOF direction is opposite that of surfaces that display a negative charge (anode to cathode direction).

Along with intensity profiles of pristine PETG and COO-PETG exposed to AF in the presence of EDC, is a representative fluorescence intensity profile of PETG terminated in amines (NHCH<sub>3</sub>-PETG) and exposed to AF in the presence of EDC is demonstrated in Fig. 4. As can be seen, the average fluorescence intensity profile is slightly higher than that of pristine PETG but much lower than that of COO-PETG. The reduction in fluorescence as compared to the COO-PETG may indicate successful reaction between surface carboxylate species and *N*-methyl-1,3-propane diamine because this reaction effectively “blocks” further chemical reactions involving carboxylate species. The NHCH<sub>3</sub>-PETG surface does display some fluorescence, indicating the presence of some free surface carboxylate groups. The result suggests that the reaction involving surface-bound carboxylate species and *N*-methyl-1,3-propane diamine was incomplete.

Because the reaction between the surface-bound carboxylates and *N*-methyl-1,3-propane diamine was incomplete, a decrease, but not complete reversal, in the EOF mobility of NHCH<sub>3</sub>-PETG microchannels was expected. The EOF mobility of NHCH<sub>3</sub>-PETG microchannels is  $2.67 \pm 0.6 \text{ cm}^2/\text{Vs}$ . This value is substantially less than that of COO-PETG and is quite similar to the EOF mobility obtained from pristine PETG. Thus, while the

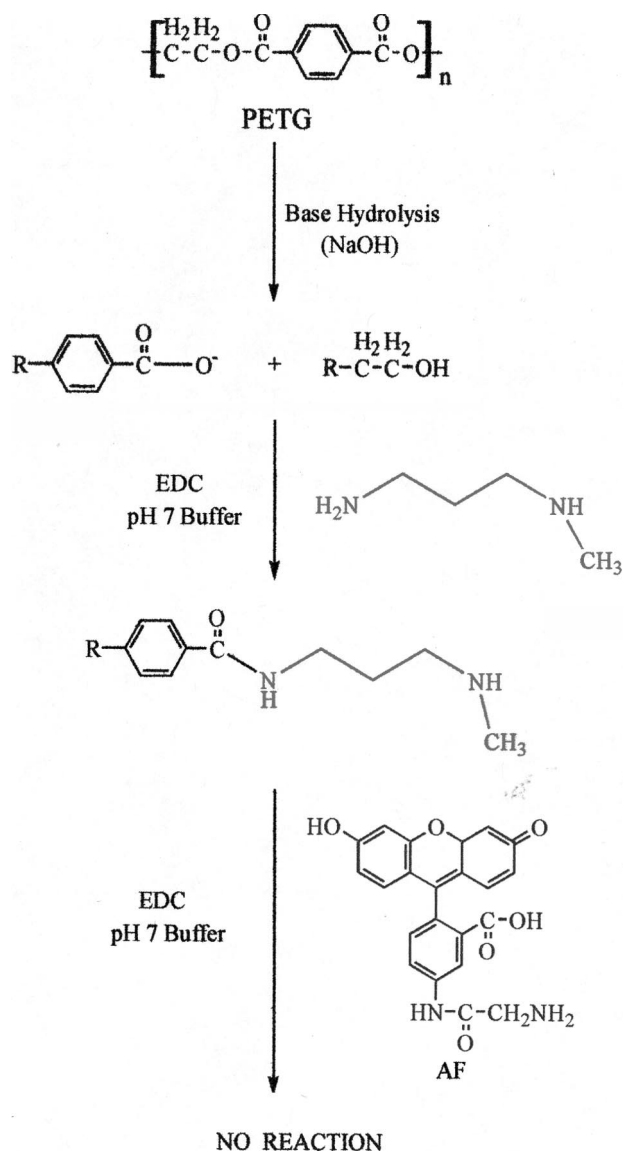


**Figure 5.** Reaction scheme of the covalent coupling of *N*-methyl-1,3-propane diamine in the presence of 1-ethyl-3-(3-dimethylaminopropyl) carbodiimide to yield NHCH<sub>3</sub>-PETG surfaces. The surface-bound secondary amines cannot be further coupled to 5-(aminoacetamido) fluorescein in the presence of 1-ethyl-3-(3-dimethylaminopropyl) carbodiimide.

direction of the EOF was not reversed upon reaction to yield a positively charged microchannel surface, the EOF mobility was slowed. In addition to the slowing of the EOF mobility, the presence of amines on the surface of the PETG microchannel will allow for the realization of still further reaction chemistries on the surface of the PETG microchannel wall. Future experiments include the implementation of more complete reaction schemes to produce amine-terminated PETG.

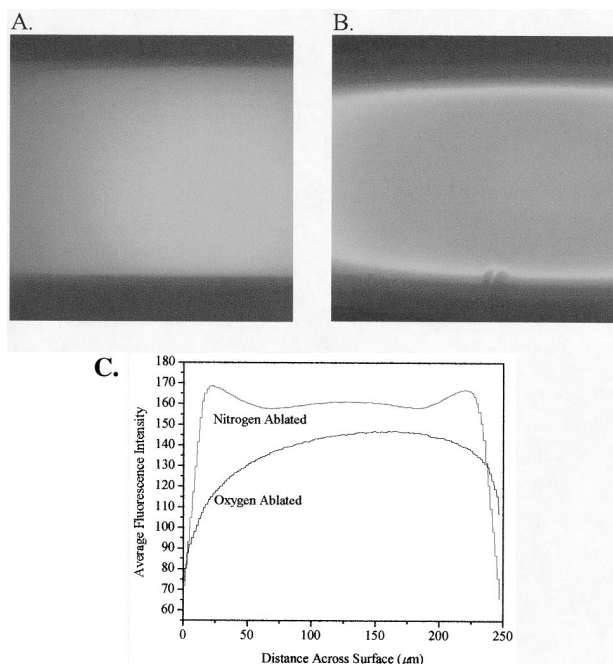


**Figure 6.** Representative fluorescence micrographs of PETG channels ablated under (A) oxygen and (B) nitrogen and then exposed to 5-(aminoacetamido) fluorescein and 1-ethyl-3-(3-dimethylaminopropyl) carbodiimide in pH 7 buffer; (C) fluorescence intensity profiles. The fluorescent portions of the images in (A) and (B) correspond to the covalent coupling of the fluorescein derivative to carboxylic acids present on the surface of the PETG. The channels were ablated at 248 nm and a laser fluence of 555 mJ/cm<sup>2</sup>.

### 3.4 Fabrication of PETG microchannels using laser ablation

Whereas the previous section explored chemical modification of preformed imprinted channels as a means to modulate EOF, it would be desirable to change the surface chemistry of the polymer during the fabrication process. This approach could possibly eliminate an additional chemical modification step during the manufacture of  $\mu$ TAS. Laser ablation has been shown to induce the formation of different functional groups on polymers [30]. Most studies involving laser ablation have been concerned with the chemical products that are pressure-ejected as part of the ablation process; however, we are concerned with the chemical moieties that remain on the surface after ablation. As with many commercial plastics, our analysis is complicated by the limited information on PETG provided by the manufacturer. Therefore, it was necessary to determine, in part, the chemical nature of the surface. In Fig. 6A and B fluorescence micrographs of PETG channels are displayed that were fabricated using the laser ablation process and then exposed to a

solution of AF and EDC in a pH 7.3 buffer. The fluorescence image and intensity profile of a microchannel ablated under an oxygen atmosphere are shown in Fig. 6A and C, respectively. The fluorescence image and intensity profile of a microchannel ablated under a nitrogen atmosphere are shown in Fig. 6B and C. As before, the fluorescent portions of the micrographs correspond to the fluorescence of AF that has been covalently coupled through an amide linkage to a surface consisting of carboxylate groups. In both cases, the images indicate that there is a higher density of carboxylates present on the ablated channels *versus* the pristine PETG surface surrounding the channel. Further, the fluorescence intensity corresponding to the PETG channel ablated under oxygen is slightly lower than that of the PETG sample ablated under nitrogen (Fig. 6C). The images indicate that the surface density of carboxylate groups on the PETG channel ablated under oxygen may be somewhat less than the density of the carboxylate groups on the channel ablated under nitrogen. However, this data is not considered to be quantitative and does not indicate the presence of other ionizable moieties.

Because of the prevalence of carboxylic acid moieties present on the surface of PETG microchannels that were laser-ablated under both oxygen and nitrogen atmospheres, one would expect the EOF to be greater than that in an imprinted (nonhydrolyzed) PETG microchannel. The EOF mobility of a PETG channel ablated under nitrogen was determined to be  $5.3 \pm 0.3 \times 10^{-4}$  cm<sup>2</sup>/Vs. Similarly, the EOF mobility of a PETG channel ablated under oxygen was found to be  $5.6 \pm 0.4 \times 10^{-4}$  cm<sup>2</sup>/Vs. One might expect, because nitrogen is much more inert than oxygen, a difference in surface chemistry between channels ablated under nitrogen *versus* channels ablated under oxygen. We do not see this trend in either the fluorescence images or in the EOF data. The EOF data indicate that there are similar numbers of ionizable groups present on the channels ablated under nitrogen and oxygen atmospheres. Interestingly, the EOF mobility of the COO-PETG imprinted channel (produced by chemical modification) was determined to be  $5.1 \pm 0.4 \times 10^{-4}$  cm<sup>2</sup>/Vs, which is similar to the values obtained for ablated channels. The surfaces are currently being studied using infrared spectroscopic and X-ray photoelectron spectroscopic methods of analysis to validate our results.

### 3.5 Chemical modification of laser-ablated PETG microchannels to yield amine-terminated ablated microchannels

It has been shown that, after exposing carboxylate-terminated PETG microchannels to *N*-methyl-1,3-propane diamine in the presence of EDC, the EOF mobility of the

channel decreased substantially. Similarly, the exposure of ablated microchannels to *N*-methyl-1,3-propane diamine in the presence of EDC resulted in microchannels that supported an EOF of  $3.38 \pm 0.1 \text{ cm}^2/\text{Vs}$ . This EOF mobility value is much decreased from that of ablated channels that had not been further chemically modified; however, as with the hydrolyzed imprinted channels, the reaction appeared to be incomplete since the direction of the EOF was not reversed. Future studies will include the implementation of more complete reaction pathways.

#### 4 Concluding remarks

The goal of this work was to demonstrate that the EOF mobility of bulk solution through a plastic microfluidic device can be altered through the use of chemical modification techniques or by merely fabricating the channel in such a manner that the surface possesses charged chemical moieties. One chemical modification technique that we have investigated involved base hydrolysis; an alternative fabrication procedure involved laser ablation. In both cases, carboxylate groups were abundant on the surfaces of the microchannels. PETG microchannels that were not hydrolyzed exhibited an EOF mobility value lower than those that were hydrolyzed by immersion in NaOH or those that were laser ablated. In addition, surface-bound carboxylic acids that were present on both hydrolyzed and ablated PETG microchannels were accessible for reactions with amines to yield microchannels terminated in secondary amines. Future experiments include the further chemical modification of surface-bound carboxylic acids and amines on chemically modified imprinted or laser ablated PETG microchannels as well as the implementation of various atmospheres under which PETG and other plastics may be ablated.

*The authors wish to thank Scott A. Wight and John Small for the acquisition of the scanning electron micrographs of the PETG microchannels and Michael Gaitan for the fabrication of the silicon templates. The authors also wish to thank David Ross for programming the analysis of current monitoring data. In addition, the financial support of the National Research Council/National Institute of Standards and Technology Postdoctoral Research Program is greatly appreciated.*

*Certain commercial equipment, instruments, or materials are identified in this report to specify adequately the experimental procedure. Such identification does not imply recommendation or endorsement by the National Institute of Standards and Technology, nor does it imply that the materials or equipment identified are necessarily the best available for the purpose.*

Received September 17, 2001

#### 5 References

- [1] Culbertson, C. T., Jacobson, S. C., Ramsey, J. M., *Anal. Chem.* 2000, 72, 5814–5819.
- [2] Jacobson, S. C., Hergenroder, R., Koutny, L. B., Ramsey, J. M., *Anal. Chem.* 1994, 66, 1114–1118.
- [3] Harrison, D. J., Manz, A., Fan, Z. H., Ludi, H., Widmer, H. M., *Anal. Chem.* 1992, 64, 1926–1932.
- [4] Chiem, N., Harrison, D. J., *Anal. Chem.* 1997, 69, 373–378.
- [5] Ramsey, R. S., Ramsey, J. M., *Anal. Chem.* 1997, 69, 1174–1178.
- [6] Meng, Z. J., Qi, S. Z., Soper, S. A., Limbach, P. A., *Anal. Chem.* 2001, 73, 1286–1291.
- [7] Giordano, B. C., Ferrance, J., Swedberg, S., Huhmer, A. F. R., Landers, J. P., *Anal. Biochem.* 2001, 291, 124–132.
- [8] Bavykin, S. G., Akowski, J. P., Zakhariiev, V. M., Barsky, V. E., Perov, A. N., Mirzabekov, A. D., *Appl. Environm. Microbiol.* 2001, 67, 922–928.
- [9] Lim, J. T., Zare, R. N., Bailey, C. G., Rakestraw, D. J., Yan, C., *Electrophoresis* 2000, 21, 737–742.
- [10] McCormick, R. M., Nelson, R. J., Alonso-Amigo, M. G., Benvegny, J., Hooper, H. H., *Anal. Chem.* 1997, 69, 2626–2630.
- [11] Henry, A. C., Tutt, T. J., Galloway, M., Davidson, Y. Y., McWhorter, C. S., Soper, S. A., McCarley, R. L., *Anal. Chem.* 2000, 72, 5331–5337.
- [12] Soper, S. A., Ford, S. M., Qi, S., McCarley, R. L., Kelly, K., Murphy, M. C., *Anal. Chem.* 2000, 72, 642A–651A.
- [13] Ford, S. M., Davies, J., Kar, B., Qi, S. D., McWhorter, S., Soper, S. A., Malek, C. K., *J. Biomech. Engineer.* 1999, 121, 13–21.
- [14] Martynova, L., Locascio, L. E., Gaitan, M., Kramer, G. W., Christensen, R. G., Maccreehan, W. A., *Anal. Chem.* 1997, 69, 4783–4789.
- [15] Xu, J., Locascio, L. E., Gaitan, M., Lee, C. S., *Anal. Chem.* 2000, 72, 1930–1933.
- [16] Becker, H., Gärtner, C., *Electrophoresis* 2000, 21, 12–26.
- [17] Becker, H., Heim, U., *Sensors and Materials* 1999, 11, 297–304.
- [18] Roberts, M. A., Rossier, J. S., Bercier, P., Girault, H. H., *Anal. Chem.* 1997, 69, 2035–2042.
- [19] Ruano, J. M., Benoit, V., Aitchison, J. S., Cooper, J. M., *Anal. Chem.* 2000, 72, 1093–1097.
- [20] Johnson, T. J., Ross, D., Gaitan, M., Locascio, L. E., *Anal. Chem.* 2001, 73, 3656–3661.
- [21] Ross, D., Johnson, T. J., Locascio, L. E., *Anal. Chem.* 2001, 73, 2509–2515.
- [22] Barker, S. L. R., Tarlov, M. J., Canavan, H., Hickman, J. J., Locascio, L. E., *Anal. Chem.* 2000, 72, 4899–4903.
- [23] Barker, S. L. R., Ross, D., Tarlov, M. J., Gaitan, M., Locascio, L. E., *Anal. Chem.* 2000, 72, 5925–5929.
- [24] Bianchi, F., Chevolut, Y., Mathieu, H. J., Girault, H. H., *Anal. Chem.* 2001, 73, 3845–3853.
- [25] Bianchi, F., Wagner, F., Hoffmann, P., Girault, H. H., *Anal. Chem.* 2001, 73, 829–836.
- [26] Johnson, T. J., Waddell, E. A., Kramer, G. W., Locascio, L. E., *Appl. Surface Sci.* 2001, 149–159.
- [27] Branham, M. L., MacCrehan, W. A., Locascio, L. E., *J. Capil. Electrophor. Microchip Technol.* 1999, 43–50.
- [28] Locascio, L. E., Perso, C. E., Lee, C. S., *J. Chromatogr. A* 1999, 857, 275–284.
- [29] Wang, S. C., Perso, C. E., Morris, M. D., *Anal. Chem.* 2000, 72, 1704–1706.
- [30] Srinivasan, R., Braren, B., *J. Polymer Sci. A* 1984, 22, 2601–2609.